

THE 5 HR PULSE PERIOD AND BROADBAND SPECTRUM OF THE SYMBIOTIC X-RAY BINARY 3A 1954+319

DIANA M. MARCU^{1,2}, FELIX FÜRST³, KATJA POTTSCHMIDT^{1,2}, VICTORIA GRINBERG³, SEBASTIAN MÜLLER³, JÖRN WILMS³, KONSTANTIN A. POSTNOV⁴,
ROBIN H. D. CORBET^{5,2}, CRAIG B. MARKWARDT⁵, AND MARION CADOLLE BEL⁶

Accepted October 18, 2011

ABSTRACT

We present an analysis of the highly variable accreting X-ray pulsar 3A 1954+319 using 2005–2009 monitoring data obtained with *INTEGRAL* and *Swift*. This considerably extends the pulse period history and covers flaring episodes in 2005 and 2008. In 2006 the source was identified as one of only a few known symbiotic X-ray binaries (SyXBs), i.e., systems composed of a neutron star accreting from the inhomogeneous medium around an M-giant star. The extremely long pulse period of ~ 5.3 hr is directly visible in the 2008 *INTEGRAL*-ISGRI outburst light curve. The pulse profile is double peaked and generally not significantly energy dependent although there is an indication of possible softening during the main pulse. During the outburst a strong spin-up of -1.8×10^{-4} hr hr⁻¹ occurred. Between 2005 and 2008 a long-term spin-down trend of 2.1×10^{-5} hr hr⁻¹ was observed for the first time for this source. The 3–80 keV pulse peak spectrum of 3A 1954+319 during the 2008 flare could be well described by a thermal Comptonization model. We interpret the results within the framework of a recently developed quasi-spherical accretion model for SyXBs.

Subject headings: binaries: symbiotic — stars: individual (3A 1954+319) — stars: neutron — X-rays: binaries

1. INTRODUCTION

The X-ray source 3A 1954+319 was detected in the Cygnus region in surveys by *Uhuru*, *Ariel V*, *EXOSAT*, and *ROSAT* (Forman et al. 1978; Warwick et al. 1981, 1988; Voges et al. 1999). Pointed observations with *EXOSAT* (Cook et al. 1985) and *Ginga* (Tweedy et al. 1989) showed a hard X-ray spectrum as well as intensity variations by an order of magnitude on timescales of minutes. This led to the suggestion that the system might be a High Mass X-ray Binary (HMXB). Only when Masetti et al. (2006) identified the companion as an M4–M5 III star at a distance of $\lesssim 1.7$ kpc and Corbet et al. (2006) discovered a ~ 5 hr pulse period in early *Swift*-BAT data, did it become clear that 3A 1954+319 is a Symbiotic X-ray Binary (SyXB). SyXBs constitute a small group⁷ of persistent Low Mass X-ray Binaries (LMXBs) in which a neutron star is orbiting in the inhomogeneous medium around an M-type giant star⁸.

SyXBs typically have wide orbits, e.g., the prototype GX 1+4 has an orbital period of ~ 1161 days (Hinkle et al. 2006). Their X-ray emission is therefore due to wind accretion, a process not well investigated for late type donors. Two

broadband spectral studies support the SyXB interpretation for 3A 1954+319: Mattana et al. (2006) modeled the non-simultaneous *BeppoSAX* and *INTEGRAL* spectrum with a highly absorbed ($N_{\text{H}} \sim 10^{23}$ cm⁻²) cutoff power law with a photon index of 1.1 and a folding energy of 15 keV and a weak Fe K α line. These authors also confirmed the detection of the ~ 5 hr period in BAT and ISGRI data. In a study of archival data spanning absorbed 2–10 keV luminosities from 3.4×10^{34} erg s⁻¹ to 1.8×10^{35} erg s⁻¹ Masetti et al. (2007) confirmed the empirical spectral description for the > 2 keV spectrum and determined a best fit using thermal Comptonization, modified by complex absorption (ionized plus partially covering neutral absorption). They also modeled a < 2 keV soft excess with a ~ 50 eV hot plasma and interpreted it, together with the two-zone absorption, as being due to a diffuse, partly ionized cloud of material around the neutron star.

The ~ 5 hr period is the only period known for this system. As Corbet et al. (2006, 2008) argued (i) the period value itself is inconsistent with being the orbital period of an M-giant, (ii) the large period decline of $(2.6 \pm 0.2) \times 10^{-5}$ hr hr⁻¹ observed over the first year of BAT data cannot be due to orbital Doppler modulation, and (iii) the period change is also too large to be supported by a white dwarf accretor. Interpreting the ~ 5 hr period as a neutron star spin period makes 3A 1954+319 the slowest rotating neutron star in an X-ray binary currently known and one of the slowest pulsars in general – with only the 6.67 hr pulsar in the supernova remnant RCW 103 showing a larger value (De Luca et al. 2006). Corbet et al. (2008) also noted that if the neutron star rotated close to its equilibrium period for disk accretion, as usually assumed in accreting sources, the long period would imply a neutron star magnetic field of $\sim 10^{15}$ G rather than of $\sim 10^{12}$ G. The latter value is more commonly observed for accreting pulsars and is consistent with a spin-down origin of the long period (Mattana et al. 2006). From the *Swift*-BAT and *RXTE*-ASM data available at the time it was not clear whether the strong spin-up observed was associated with the long flaring episode in 2005 and/or whether the source might show a spin-down at lower fluxes, as it is the case for GX 1+4 (Corbet et al. 2008).

¹ NASA Goddard Space Flight Center, Astrophysics Science Division, Code 661, Greenbelt, MD 20771, USA

² CRESST & University of Maryland Baltimore County, 1000 Hilltop Circle, Baltimore, MD 21250, USA

³ Dr. Karl Remeis-Observatory & ECAP, University of Erlangen-Nuremberg, Sternwartstr. 7, 96049 Bamberg, Germany

⁴ Sternberg Astronomical Institute, 119992, Moscow, Russia

⁵ NASA Goddard Space Flight Center, Astrophysics Science Division, Code 662, Greenbelt, MD 20771, USA

⁶ European Space Agency, European Space Astronomy Centre P.O. Box 78, 28691 Villanueva de la Cañada, 28692, Madrid, Spain

⁷ In addition to 3A 1954+319 a recent list of SyXB given by Nespoli et al. (2010) consists of: GX 1+4, 4U 1700+24, Scutum X-1, IGR J16194–2810, 1RXS J180431.1–273932, IGR J16358–4726, and IGR J16393–4643. Note that the X-ray mass function of IGR J16393–4643 argues against a LMXB classification, though (Pearlman et al. 2011).

⁸ The classification is related to but not identical to that of “Symbiotic Binaries”, systems consisting of a white dwarf and a red giant. The latter were named after their optical spectra which show contributions from both binary components, different from SyXBs where the neutron star is not visible at optical wavelengths.

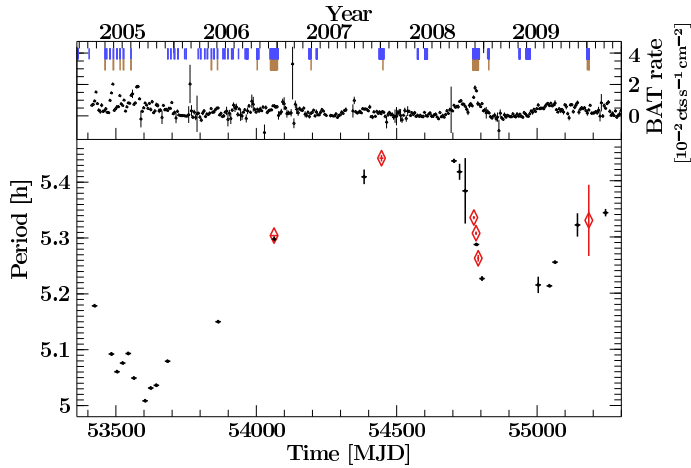


Figure 1. From top to bottom: *INTEGRAL* observations of 3A 1954+319 with an offset angle $\leq 10^\circ$ and *INTEGRAL*-ISGRI detections (blue and brown tickmarks, respectively). The long-term light curve shown was obtained by *Swift*-BAT in the 15–50 keV range and has been rebinned to a resolution of 5 days. The lower part of the figure shows the pulse period evolution as determined by BAT (black) and ISGRI (red).

(A color version of this figure is available in the online journal.)

In this Letter we considerably extend the pulse period history for 3A 1954+319 and present a timing and spectral analysis of a flaring episode in 2008 (Fürst et al. 2011 presented a preliminary analysis of these data). Section 2 describes the observations and data reduction. Section 3 reports the results, including long-term and high time resolution light curves, energy resolved pulse profiles, the pulse period evolution, and the broadband spectrum. In Section 4 the results are summarized and discussed.

2. OBSERVATIONS AND DATA REDUCTION

The upper part of Figure 1 shows the 2005–2009 15–50 keV light curve of 3A 1954+319⁹ observed with *Swift*-BAT (Barthelmy et al. 2005). Months long flaring episodes are apparent, especially in 2005 and in 2008. The former includes most of the time range analyzed by Corbet et al. (2008), \sim MJD 53330–53680. The short tickmarks above the BAT light curves indicate 1163 *INTEGRAL* (Winkler et al. 2003) pointings (“science windows”, \sim 2 ks exposures) during which 3A 1954+319 was within the field of view of the ISGRI (Lebrun et al. 2003) of the IBIS instrument, with a pointing offset $\leq 10^\circ$.

Since its launch in 2002 *INTEGRAL* has performed several extensive monitoring campaigns of the Cygnus region (Pottschmidt et al. 2003; Cadolle Bel et al. 2006; Martin et al. 2009; Laurent et al. 2011; Williams et al. 2011). A Key Program (KP) centered on the black hole X-ray binary Cygnus X-1, located $3^\circ.15$ from 3A 1954+319, has been in place since 2008 with annual exposures of several 100 ks (Grinberg et al. 2011). Coincidentally these KP observations covered about three weeks of the 2008 flare of 3A 1954+319 in unprecedented detail (Figure 1).

The 201 science windows for which 3A 1954+319 was detected (OSA DETSIG ≥ 6 in the 20–100 keV science window images) are indicated by long tickmarks in Figure 1. For these pointings the `ii_light` tool in version 7 of the Offline Scientific Analysis (OSA; Courvoisier et al. 2003)¹⁰ was applied to

⁹ Daily light curve from <http://heasarc.gsfc.nasa.gov/docs/swift/results/transients/4U1954p31/>.

¹⁰ The `ii_light` tool was not present in OSA 8 and at the time of writing

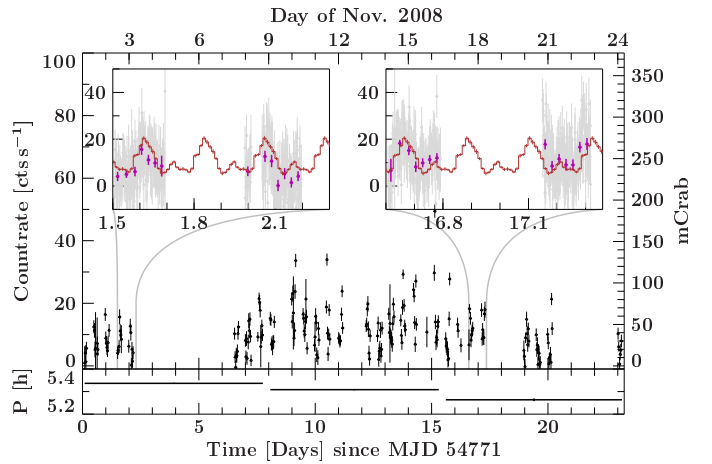


Figure 2. Upper panel: *INTEGRAL*-ISGRI 20–100 keV light curve of 3A 1954+319 observed during the flaring episode in 2008. Each data point represents one science window (\sim 2 ks). The insets show two close-ups with the full 100 s resolution light curve (gray), the count rates per science window (magenta), and the average pulse profile (red histogram). Lower panel: The three pulse period measurements obtained with ISGRI during the flare.

(A color version of this figure is available in the online journal.)

produce ISGRI light curves of 3A 1954+319 with a time resolution of 100 s in the energy bands 20–40 keV, 40–100 keV, and 20–100 keV. Together with the BAT long-term light curve the 20–100 keV ISGRI light curves were used to determine the pulse period evolution (Section 3.3).

In addition, a more detailed analysis was performed for the flare in 2008. This dataset included science windows from satellite revolutions 739, 741–746, 756, and 758 (one revolution takes about three days). Pulse profiles in the three energy bands were created (Section 3.2). In order to maximize the signal to noise ratio (S/N) all science windows in the phase range of 0.45–0.85, i.e., associated with the main pulse peak, were selected. OSA 9 was used to extract average ISGRI and Joint European X-ray Monitor (JEM-X; Lund et al. 2003) spectra, for source offset angles $\leq 10^\circ$ and $\leq 3^\circ$, respectively. The ISGRI spectrum had an exposure of 85 ks, was created by averaging spectra from individual science windows, and was modeled in the 20–80 keV range. The JEM-X spectrum had an exposure of 9.8 ks, was extracted from mosaic images using `mosaic_spec` and was modeled in the 3–30 keV range (Section 3.4). Response and auxiliary response files were selected or created following the analysis documentation¹¹.

3. RESULTS

3.1. Light Curves

The long-term BAT light curve shown in Figure 1 demonstrates the irregular flaring of 3A 1954+319 on timescales of months, with the 2008 November flare having been one of the brightest since the start of the BAT monitoring. The *INTEGRAL* observations cover the second half of the flaring episode. The resulting 20–100 keV ISGRI light curve is shown in the upper panel of Figure 2. The 20–100 keV flux during the outburst varied by a factor of \sim 20 with an average of \sim 40 mCrab and a peak value of \sim 130 mCrab.

The insets of Figure 2 show close-ups of two randomly selected parts of the ISGRI outburst light curve with a resolution of 100 s. Individual pulses are directly observed in the light curve for the first time. Also shown are repetitions of the

was still undergoing evaluation for OSA 9.

¹¹ See <http://www.isdc.unige.ch/integral/analysis#Documentation>

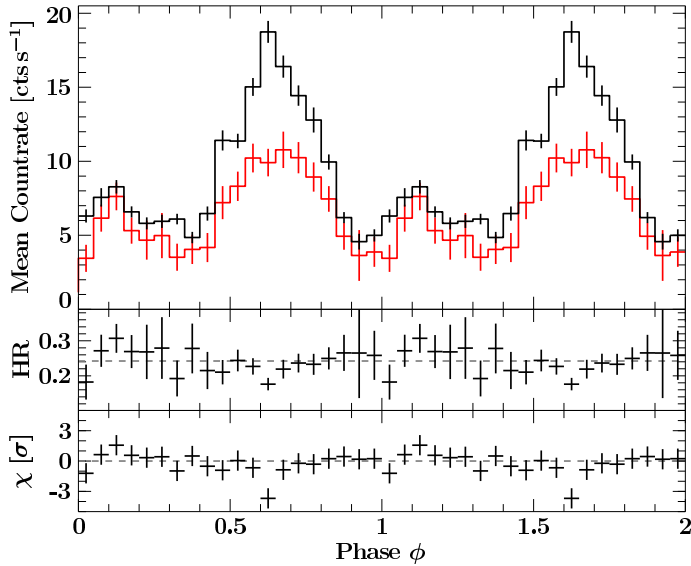


Figure 3. Upper panel: ISGRI pulse profiles for the flaring episode in 2008, in the energy ranges of 20–40 keV (black) and 40–100 keV (red, multiplied by 3 for better visibility). Middle panel: Hardness ratio obtained by dividing the 40–100 keV by the 20–40 keV profile. The dashed line indicates the mean hardness. Lower panel: Deviation of the hardness ratio from the mean hardness in units of σ . The dashed line indicates no deviation. (A color version of this figure is available in the online journal.)

\dot{P} -corrected average pulse profile obtained by folding the high resolution light curve on the pulse ephemeris determined from the outburst data (Section 3.3). Comparing the profiles with the high time resolution light curve and the average science window count rates demonstrates general consistency but allows for moderate pulse-to-pulse variations which are common in accreting X-ray pulsars (Klochkov et al. 2011).

3.2. Pulse Profiles

Pulse profiles in the energy ranges of 20–40 keV and 40–100 keV were obtained by folding the energy resolved high time resolution ISGRI outburst light curves on the pulse ephemeris determined from the 2008 outburst data (Section 3.3), see upper panel of Figure 3. These are the highest quality pulse profiles available for the source to date. They clearly show a double peaked structure, in contrast to the single peaked pulse profile displayed by the prototype SyXB GX 1+4 (Ferrigno et al. 2007). While the possible presence of the secondary peak for 3A 1954+319 was indicated in the <50 keV BAT profiles presented by Corbet et al. (2008), it could not be detected in the 50–100 keV band, possibly due to the comparatively smaller S/N. The lower two panels of Figure 3 show the hardness ratio between the profiles in the two energy bands and its deviation from the average ratio. No significant energy dependence was detected with exception of a possible moderate softening during the brightest part of the main pulse in a narrow phase range ($\sim 0.60 - 0.65$).

3.3. Pulse Period Evolution

Using the epoch folding technique (Schwarzenberg-Czerny 1989) pulse period values were determined for three equally long parts of the 2008 outburst observations with ISGRI. The results are shown in the lower panel of Figure 2. Uncertainties were calculated according to the Monte Carlo method described by Davies (1990): for every segment 10^4 light curves with the same sampling and variance as seen in the observational data were simulated, based on the segment's average

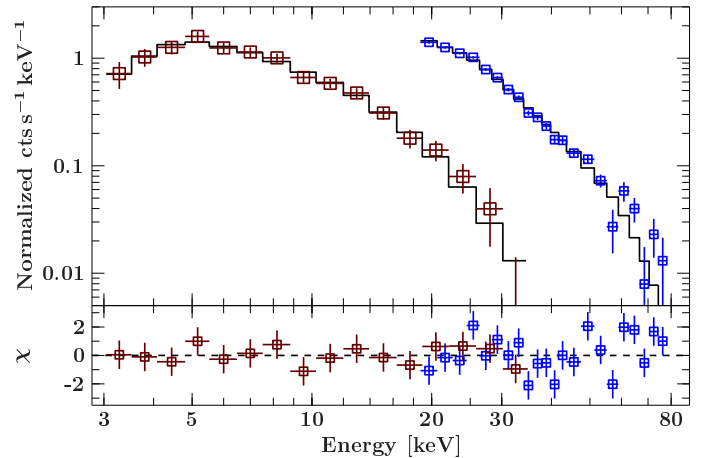


Figure 4. Upper panel: JEM-X (3–30 keV, brown) and ISGRI (20–80 keV, blue) counts spectra for the flaring episode in 2008. In order to obtain a better S/N only data from the main pulse, i.e., phases 0.45–0.85, were included. The best fit description consisted of an absorbed thermal Comptonization model and is also displayed. Lower panel: Best fit residuals.

(A color version of this figure is available in the online journal.)

pulse profile modified by Gaussian noise. A successful period search was performed for every simulated light curve and the widths of the emerging distributions were used as uncertainties of the pulse period measurements. The three ISGRI pulse period values for the flare evolved from 5.336 ± 0.003 hr over 5.308 ± 0.003 hr to 5.264 ± 0.006 hr, i.e., a strong spin-up became apparent. The pulse ephemeris over the 2008 flare was determined to $T_0 = \text{MJD}54782.6897$, $P(T_0) = 5.3060 \pm 0.0007$ hr, and $\dot{P}(T_0) = (-1.81 \pm 0.17) \times 10^{-4}$ hr hr $^{-1}$ (uncertainties are given on a 1σ confidence level).

In order to put the ISGRI period values into perspective the pulse period history from the long-term BAT light curve was updated by performing local period determinations for 20 days long segments. The lower part of Figure 1 contains all successful BAT period measurements, the three ISGRI flare measurements, as well as three additional ISGRI measurements that could typically be obtained during times of denser sampling and/or elevated count rates¹². The long-term results are the following: (i) the spin-up phase during the flaring activity in 2005, analyzed by Corbet et al. (2008) and Mattana et al. (2006), was reproduced, (ii) it was followed by a long spin-down trend between 2005 and 2008, characterized by $\dot{P} \sim 2.1 \times 10^{-5}$ hr hr $^{-1}$, (iii) the BAT and ISGRI pulse period values are in excellent agreement, especially during the strong spin-up in 2008, (iv) the spin-down trend resumed in 2009, possibly slowed down by continued moderate flaring. Note that while the possibility of a beginning spin-down at the end of 2005 was mentioned by Corbet et al. (2008), a spin-down has now been clearly observed for the first time for 3A 1954+319. Also note that the spin-up in 2008 was an order of magnitude larger than the one in 2005.

3.4. Broadband Spectrum

As described above the 3–80 keV spectrum of 3A 1954+319 was determined for the phase range associated with the peak of the main pulse. This approach was chosen because the source is close to the detection limit during dimmer pulse phases. The spectrum could be well

¹² Following a conservative approach only peaks which were visually clearly apparent in the epoch folding statistics were selected.

described by an absorbed thermal Comptonization model (Figure 4), resulting in $\chi^2_{\text{red}} = 1.3$ for 32 degrees of freedom. The best fit parameters obtained were $N_{\text{H}} = 3.9^{+6.7}_{-2.2} \times 10^{22} \text{ cm}^{-2}$, $kT_0 = 0.9^{+0.4}_{-0.9} \text{ keV}$, $\tau = 4.2 \pm 0.7$, and $kT_e = 7.5^{+0.5}_{-0.4} \text{ keV}$. A flux cross calibration factor of $0.84^{+0.12}_{-0.11}$ was applied to model the JEM-X data. The residuals mainly reflect known ISGRI calibration uncertainties (Grinberg et al. 2011). All fit parameter uncertainties, including those of the flux measurements below, are given at the 90% level for one interesting parameter. A broken power law fit provided a slightly better description but the improvement is due to masking cross-calibration issues ($\chi^2 \sim 1.2$). A cutoff power law model as applied by Mattana et al. (2006) resulted in a worse fit ($\chi^2 \sim 1.9$).

The absorbed 2–10 keV and 10–100 keV fluxes were $7.2^{+0.8}_{-0.7}$ and $12.1^{+0.3}_{-0.3} \times 10^{-10} \text{ erg cm}^{-2} \text{ s}^{-1}$, respectively (ISGRI normalization). The unabsorbed fluxes were $9.1^{+2.7}_{-2.0}$ and $12.2^{+0.4}_{-0.3} \times 10^{-10} \text{ erg cm}^{-2} \text{ s}^{-1}$, corresponding to (pulse peak) luminosities of 3.1 and $4.2 \times 10^{35} \text{ erg s}^{-1}$ for a distance of 1.7 kpc. Since the assumed distance is an upper limit (Masetti et al. 2006), these luminosities are upper limits as well. They are comparable to the highest luminosities reported by Masetti et al. (2007).

4. DISCUSSION

A possible scenario for the development of pulse periods longer than a few hundred seconds has been proposed for persistently bright HMXBs by Ikhsanov (2007), where accretion proceeds spherically and a strong spin-down happened in a previous accretion epoch (subsonic propeller regime). The author argues that the 2.7 hr pulse period of the HMXB 2S 0114+650 (Farrell et al. 2008) can thus be explained without the need for an unusually high (10^{15} G) magnetic field.

For the LMXB 3A 1954+319 the long pulse period is more easily reconcilable with the system’s life time (Mattana et al. 2006). Shakura et al. (2011) recently developed an accretion model for SyXBs that can not only account for long spin periods but also provides a mechanism allowing for quasi-spherical accretion. In this model a subsonic settling regime occurs for X-ray luminosities below $\sim 3 \times 10^{36} \text{ erg s}^{-1}$, i.e., for luminosities consistent with those observed for 3A 1954+319. A shell of hot material forms around the magnetosphere which mediates the transfer of angular momentum to/from the neutron star by advection and viscous stress. The accretion rate is determined by the ability of the plasma to enter the magnetosphere. The equilibrium pulse period in this case is:

$$\frac{P_{\text{eq}}}{10^3 \text{ s}} \sim \left(\frac{B}{10^{12} \text{ G}} \right)^{12/11} \left(\frac{P_{\text{orbit}}}{10 \text{ d}} \right) \left(\frac{L_{\text{X}}}{10^{36} \text{ erg s}^{-1}} \right)^{4/11} \left(\frac{v_{\text{wind}}}{10^3 \text{ km s}^{-1}} \right)^4 \quad (1)$$

where P_{orbit} is the binary period and v_{wind} is the stellar wind velocity with respect to the neutron star. Reporting on population synthesis simulations for SyXBs based on this model, Postnov et al. (2011) showed that the 5.3 hr pulse period of 3A 1954+319 can be well reproduced.

3A 1954+319 seems to show long spin-down episodes between major flares ($\dot{P} \sim 2.1 \times 10^{-5} \text{ hr hr}^{-1}$) which are reminiscent of the spin-down displayed by GX 1+4 since the early 1980s ($\dot{P} \sim 10^{-7} \text{ hr hr}^{-1}$; González-Galán et al. 2011). Several models beyond equilibrium disk accretion have been proposed to explain the spin-down of GX 1+4 without invoking unusually high magnetic fields, for example the presence of a counterrotating disk (Nelson et al. 1997) or accretion of fall-

back material expelled during the propeller phase (Perna et al. 2006). Only the quasi-spherical accretion model, however, reproduces the correct sign and magnitude of the negative correlation between spin frequency change $\dot{\nu}$ and X-ray flux F_{X} observed during spin-down in this source ($-\dot{\nu} \propto F_{\text{X}}^{3/7}$; González-Galán et al. 2011). For 3A 1954+319 such a detailed study of the $\dot{\nu}$ - F_{X} -relationship is difficult, especially during spin-down since the low flux allowed for only a few $\dot{\nu}$ measurements (Figure 1). It is beyond the scope of this Letter.

On longer time scales we observe torque reversals and a positive $\dot{\nu}$ - F_{X} -correlation between low (spin-down) and high flux (spin-up) episodes (Figure 1). This is consistent with the behavior predicted by the quasi-spherical accretion model for higher accretion rates within the settling regime (see Figure 1 of Shakura et al. 2011).

The strong spin-up in 2008 translates to $\dot{P}/P = -0.9 \times 10^{-8} \text{ s}^{-1}$. While still high, the absolute value is of the same order of magnitude as the spin-down related \dot{P}/P of $3.1 \times 10^{-8} \text{ s}^{-1}$ observed for the SyXB IGR J16358–4724 (Patel et al. 2007). The X-ray luminosity required to sustain such a spin-up in 3A 1954+319 in the equilibrium disk accretion case would be $\sim 5 \times 10^{36} \text{ erg s}^{-1}$ (Joss & Rappaport 1984), whereas we obtained an upper limit for the pulse peak flux value of $\sim 7.4 \times 10^{35} \text{ erg s}^{-1}$, again arguing against disk accretion.

This conclusion does not change when the possible contribution of a spin-up due to orbital motion is considered: According to Dumm et al. (1998) the measured maximum mass for M giants is $\sim 3.5 M_{\odot}$ and the median stellar radii determined for M4 III and M5 III stars are $103 R_{\odot}$ and $120 R_{\odot}$, respectively. For neutron star orbits outside of the M giant, the orbital period then has to be $\gtrsim 80$ days and $\gtrsim 100$ days, translating into a maximum relative change of the pulse period over the orbit of $\lesssim 4 \times 10^{-4}$ in both cases. The lowest relative uncertainty range of our pulse period measurements is $\sim 10^{-3}$, considerably bigger than any realistic orbital effect, which will be even smaller than the value above due to a typically lower stellar mass and wider orbit. Therefore the orbital influence is negligible for the 2008 spin-up measurement.

The best fit to the broadband spectrum of the 2008 flare describes an optically thick Compton plasma ($\tau = 4.2 \pm 0.7$, $kT_e = 7.5^{+0.5}_{-0.4} \text{ keV}$) with parameters qualitatively consistent with the results of Masetti et al. (2007). As these authors state the parameters are similar to those commonly seen in LMXBs with an accreting neutron star companion. Most of those sources do not show pulsations, however, and their accretion geometry is most likely different from that of pulsars. Other SyXBs show similar spectra, especially GX 1+4 ($\tau = 6.80 \pm 0.15$, $kT_e = 13.1 \pm 0.2 \text{ keV}$; Ferrigno et al. 2007). Furthermore, optically thick Comptonization has also been used to describe the emission from the accretion columns of accreting pulsars in HMXBs, e.g., for the cyclotron line source 1A 1118–61 (Suchy et al. 2011). We tentatively propose a similar origin close to the neutron star surface for the broadband X-ray emission of 3A 1954+319.

We thank the anonymous referee for useful comments. DMM and KP acknowledge NASA grants NNX08AE84G, NNX08AY24G, and NNX09AT28G. FF acknowledges support from the DAAD and thanks the NASA-GSFC for its hospitality. The work by KAP is partially supported through RFBR grant 10-02-00599. This research has been partly funded by the European Commission under contract

ITN215212 “Black Hole Universe” and by the Bundesministerium für Wirtschaft und Technologie under DLR grants 50OR0808 and 50OR1007. It is based on observations with *INTEGRAL*, an ESA project with instruments and science data centre funded by ESA member states (especially the PI countries: Denmark, France, Germany, Italy, Switzerland, Spain), Czech Republic and Poland, and with the participation of Russia and the USA. We thank the *INTEGRAL* mission planners for careful scheduling of the Cygnus region Key Program. We also thank Hans Krimm and the *Swift*-BAT team for making the *Swift*-BAT light curves available.

Facilities: *INTEGRAL*, *Swift*.

REFERENCES

- Barthelmy, S. D., Barbier, L. M., Cummings, J. R., et al. 2005, *Space Sci. Rev.*, 120, 143
- Cadolle Bel, M., Sizun, P., Goldwurm, A., et al. 2006, *A&A*, 446, 591
- Cook, M. C., Warwick, R. S., & Watson, M. G. 1985, in *X-ray Astronomy '84*, ed. M. Oda & R. Giacconi, (Komaba: Inst. Space Astronaut. Sci.), 225
- Corbet, R., Barbier, L., Barthelmy, S., et al. 2006, *ATel*, 797
- Corbet, R. H. D., Sokoloski, J. L., Mukai, K., Markwardt, C. B., & Tueller, J. 2008, *ApJ*, 675, 1424
- Courvoisier, T. J.-L., Walter, R., Beckmann, V., et al. 2003, *A&A*, 411, L53
- Davies, S. R. 1990, *MNRAS*, 244, 93
- De Luca, A., Caraveo, P. A., Mereghetti, S., Tiengo, A., & Bignami, G. F. 2006, *Science*, 313, 814
- Dumm, T., Schild, H. 1998, *New Astronomy*, 3, 137
- Farrell, S. A., Sood, R. K., O'Neill, P. M., & Dieters, S. 2008, *MNRAS*, 389, 608
- Ferrigno, C., Segreto, A., Santangelo, A., et al. 2007, *A&A*, 462, 995
- Forman, W., Jones, C., Cominsky, L., et al. 1978, *ApJS*, 38, 357
- Fürst, F., Marcu, D. M., Pottschmidt, K., et al. 2011, in 8th *INTEGRAL Workshop*, The Restless Gamma-ray Universe, POS (INTEGRAL2010), (Trieste: SISSA), 17
- González-Galán, A., Kuulkers, E., Kretschmar, P., et al. 2011, in 8th *INTEGRAL Workshop*, The Restless Gamma-ray Universe, POS (INTEGRAL2010), (Trieste: SISSA), 16
- Grinberg, V., Marcu, D. M., Pottschmidt, K., et al. 2011, in 8th *INTEGRAL Workshop*, The Restless Gamma-ray Universe, POS (INTEGRAL2010), (Trieste: SISSA), 133
- Hinkle, K. H., Fekel, F. C., Joyce, R. R., et al. 2006, *ApJ*, 641, 479
- Ikhsanov, N. R., 2007, *MNRAS*, 375, 698
- Joss, P. C., & Rappaport, S. A. 1984, *ARA&A*, 22, 537
- Klochkov, D., Santangelo, A., Staubert, R., & Rothschild, R. E. 2011, in 8th *INTEGRAL Workshop*, The Restless Gamma-ray Universe, POS (INTEGRAL2010), (Trieste: SISSA), 61
- Laurent, P., Rodriguez, J., Wilms, J., et al. 2011, *Science*, 332, 438
- Lebrun, F., Leray, J. P., Lavocat, P., et al. 2003, *A&A*, 411, L141
- Lund, N., Budtz-Jørgensen, C., Westergaard, N. J., et al. 2003, *A&A*, 411, L231
- Martin, P., Knödseder, J., Diehl, R., & Meynet, G. 2009, *A&A*, 506, 703
- Masetti, N., Orlandini, M., Palazzi, E., Amati, L., & Frontera, F. 2006, *A&A*, 453, 295
- Masetti, N., Rigon, E., Maiorano, E., et al. 2007, *A&A*, 464, 277
- Mattana, F., Götz, D., Falanga, M., et al. 2006, *A&A*, 460, L1
- Nelson, R. W., Bildsten, L., Chakrabarty, D., et al. 1997, *ApJ*, 488, L117
- Nespoli, E., Fabregat, J., & Mennickent, R. E. 2010, *A&A*, 516, 94
- Patel, S. K., Zurita, J., Del Santo, M., et al. 2007, *ApJ*, 657, 994
- Pearlman, A. B., Corbet, R. H. D., Pottschmidt, K., & Skinner, G. K. 2011, *BAAS*, 43, 42.06
- Perna, R., Bozzo, E., & Stella, L. 2006, *ApJ*, 639, 363
- Postnov, K., Shakura, N., González-Galán, A., et al. 2011, in 8th *INTEGRAL Workshop*, The Restless Gamma-ray Universe, POS (INTEGRAL2010), (Trieste: SISSA), 15
- Pottschmidt, K., Wilms, J., Chernyakova, M., et al. 2003, *A&A*, 411, L383
- Schwarzenberg-Czerny, A., 1989, *MNRAS*, 241, 153
- Shakura, N., Postnov, K., Kochetkova, A., & Hjalmarsdotter, L. 2011, *MNRAS*, in press (arXiv:1110.3701)
- Suchy, S., Pottschmidt, K., Rothschild, R. E., et al. 2011, *ApJ*, 733, 15
- Tweedy, R. W., Warwick, R. S., & Remillard, R. 1989, in *Two Topics in X-Ray Astronomy*, ed. J. Hunt & B. Battrick, (ESA SP-296, (Noordwijk: ESA Publications Department)), 661
- Voges, W., Aschenbach, B., Boller, T., et al. 1999, *A&A*, 349, 389
- Warwick, R. S., Marshall, N., Fraser, G. W., et al. 1981, *MNRAS*, 197, 865
- Warwick, R. S., Norton, A. J., Turner, M. J. L., Watson, M. G., & Willingale, R. 1988, *MNRAS*, 232, 551
- Williams, P. K. G., Tomsick, J. A., Bodaghee, A., et al. 2011, *ApJ*, 733, L20
- Winkler, C., Courvoisier, T. J.-L., Di Cocco, G., et al. 2003, *A&A*, 411, L1